Journal of Membrane Science 465 (2014) 177–184

Contents lists available at ScienceDirect

Journal of Membrane Science

journal homepage: www.elsevier.com/locate/memsci

Consideration of a nitrogen-selective membrane for postcombustion carbon capture through process modeling and optimization

Mengyao Yuan, Kumnoon Narakornpijit, Reza Haghpanah, Jennifer Wilcox *

Department of Energy Resources Engineering, Stanford University, Stanford, CA 94305, United States

ARTICLE INFO

Article history:
Received 23 November 2013
Received in revised form
15 April 2014
Accepted 15 April 2014
Available online 23 April 2014

Keywords:
Carbon capture
Membrane separation
Metallic membrane
Multiobjective optimization
Selective nitrogen separation

ABSTRACT

The potential of a nitrogen-selective membrane for postcombustion CO_2 capture from a coal-fired power plant was investigated in this study. Bi-objective optimization was performed using the nondominated sorting genetic algorithm II (NSGA-II) to simultaneously minimize energy consumption and membrane surface area requirement with targets of $>90\%$ CO_2 capture and 95% purity. The properties of the nitrogen-selective membrane used in the calculation are based on measurements of nitrogen and hydrogen transport in vanadium at high temperatures (ca. 600 °C). The lowest energy consumption was found to be 1.1 GJ/metric ton CO_2 with a hybrid nitrogen- and CO_2-selective membrane system.

1. Introduction

Studies have indicated that increases in atmospheric CO_2 concentration have caused irreversible climate changes such as global warming and an increase in extreme weather events [1]. With the average atmospheric CO_2 level reaching 400 ppm [2], the reduction of anthropogenic CO_2 emissions is a climate change mitigation strategy long due. Currently, 30 gigatons (Gt) of CO_2 from the combustion of fossil fuels is emitted worldwide on an annual basis, and approximately 40% of the emissions come from power plants and other large stationary sources such as cement production plants and refineries [3]. Carbon capture and sequestration (CCS) is investigated as a measure to reduce CO_2 emissions from these sources [4]. In particular, postcombustion capture, or the separation of CO_2 from the flue gas after fuel combustion, has the advantage of being more easily retrofitted to existing units [5,6] and has been the focus of many studies [7]. In particular, membrane separation has been studied as a postcombustion capture technology for its advantages such as a small footprint, environmental friendliness, i.e., no solvent involved in the separation process, and energy use that is potentially competitive with amine absorption, the most developed carbon capture technology [8].

Research on modeling and optimization of postcombustion membrane separation systems has been primarily centered on polymer-based CO_2-selective technologies [5,7–20], where the CO_2 in flue gas – most often modeled as a binary mixture of CO_2 and N_2 – is preferentially permeated across the membrane and concentrated and collected in the permeate stream. Although the application of CO_2-selective membranes in postcombustion capture has shown great potential, one of the challenges this application faces is low CO_2 feed concentrations and subsequent lack of driving force for mass transfer across the membrane. CO_2 concentrations in flue gas range from 12 to 15 vol% in coal-fired power plants [3]. Besides gas compression, which is typically achieved by feed compression or permeate vacuum pumping, more sophisticated process designs such as multistage separation and stream recycling will need to be employed to achieve more stringent separation targets such as 90% capture and 95% product purity [5,15,19].

In the current study, the concept of nitrogen-selective membranes has been assessed as a postcombustion capture option. Multiobjective optimization was performed for different membrane process designs to identify the operating conditions that minimize the energy penalty and membrane surface area while meeting the stringent purity–recovery constraints for the capture unit. The concept of the nitrogen-selective membrane has been experimentally validated using pure vanadium membrane foils [21]. Although the membrane is currently under development and testing at the laboratory scale, the technical feasibility of such a membrane for industrial-level postcombustion capture applications may be worth investigating due to potential energy savings associated with CO_2 capture. In particular, two potential advantages motivated our study. First, the predominantly higher N_2

* Corresponding author. Tel.: 650 724 9449; fax: 650 725 2099.
E-mail address: jen.wilcox@stanford.edu (J. Wilcox).

http://dx.doi.org/10.1016/j.memsci.2014.04.026
0376-7388/

Table 1
Flue gas data used in the study.

		Unit
Temperature	> 1000 (from furnace) [23], 40 (from stack)	°C
Pressure	1.01	bar
Flow rate	2.1	million m^3 (STP)/hr
Composition		
N_2	69.8	mol%
H_2O	12.9	mol%
CO_2	12.2	mol%
O_2	4.3	mol%
Ar	0.8	mol%

concentration in flue gas provides a higher driving force for gas separation, where N_2 instead of CO_2 is selectively permeated across the membrane. Second, the concentrated CO_2 stream exits from the high-pressure retentate stream instead of the low-pressure permeate stream. This may displace part of the compression energy required for product compression for pipeline transport and subsequent storage.

Present optimization work on postcombustion membrane separation mostly concerns single-objective optimization on separation costs or energy use. However, a capture process should satisfy two criteria that have immediate implications for operating and capital costs, namely low parasitic energy consumption and a small footprint. In this study, multiobjective optimization was performed on nitrogen-selective membrane systems and combined nitrogen- and CO_2-selective membrane systems. Energy consumption and membrane surface area required for a 650-MW coal-fired power plant were simultaneously minimized using the built-in MATLAB function *gamultiobj*, which implements the genetic algorithm (GA) for multiobjective optimization.

2. Methodology

2.1. Reference plants and flue gas

The flue gas data for the reference plant used in this study are shown in Table 1. Unless otherwise specified, the data are based on a 650-MW_{gross} pulverized coal (PC) power plant in the Integrated Environmental Control Model (IECM) software program. IECM was developed by Professor Edward Rubin and colleagues of Carnegie Mellon University for assessing performance, emissions, and cost of fossil-fueled power plants [22]. Medium-sulfur Appalachian coal was used as the fuel for the reference plant.

The flue gas from the PC plant also contains trace components such as NO_x, SO_x, and Hg, but their impact on membrane performance was not considered in the current study. Furthermore, the flue gas was treated as a binary mixture containing ca. 15 mol% CO_2 and 85 mol% N_2. The CO_2 and N_2 concentrations were calculated from the original compositions of the flue gas streams in Table 1.

2.2. Nitrogen-selective membranes

A schematic of a nitrogen-selective membrane is shown in Fig. 1. The countercurrent flow scheme was chosen to model a tubular membrane module. The tubular membrane configuration is commonly used in hydrogen production and purification membrane units [24], which would be similar to those used in nitrogen-selective

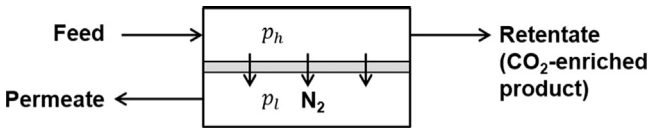

Fig. 1. Schematic diagram of a nitrogen-selective membrane.

membrane applications. In Fig. 1, the compressed feed enters at a pressure, p_h. While the feed passes along the axial direction of the membrane module, nitrogen is selectively transported through the membrane and is concentrated on the permeate side. The retentate stream, having a higher CO_2 concentration than the feed, is collected as the product.

In membrane process modeling, it is common convention to assume that the pressure drop along the axial direction of the feed side is negligible [25]. With this assumption, the product stream exits from the nitrogen-selective membrane at p_h and can be directly compressed to a higher pressure for pipeline transport. This could prevent energy loss from recompressing the product from a low pressure. In contrast, in a CO_2-selective membrane process, the product stream is the low-pressure permeate stream. Although some energy can be recovered from the expansion of the high-pressure retentate stream, the pressure increase from feed compression cannot be directly used in the compression for pipeline transport.

An ideal nitrogen-selective membrane has been modeled, in which nitrogen is transported across the membrane via a solution–diffusion mechanism, with the membrane impervious to CO_2 for two reasons: (a) the membrane has minimal defects to allow for the passage of CO_2 through Knudsen diffusion and (b) CO_2 is insoluble in the metallic materials and thus cannot be transported across the dense membrane via the solution–diffusion mechanism. Under this assumption, the N_2/CO_2 selectivity was assumed to be > 1000, and N_2 concentration in the permeate stream was assumed to approach 100%. This high selectivity is also found in H_2/CO_2 membranes, which share the same permeation mechanism with nitrogen-selective membranes [26].

The equation used to calculate the nitrogen flux in metals can be derived from combining Fick's first law of diffusion and Sieverts' law. The equation has been described in Buxbaum and Kinney's work for hydrogen transport in metals [27] and was adopted in this study for calculating the nitrogen flux:

$$J_{N_2} = \frac{P_M}{\delta}\left(\sqrt{p_h x_{N_2}} - \sqrt{p_l y_{N_2}}\right) \quad (1)$$

such that J_{N_2} is the nitrogen flux [mol/m^2 s], P_M is the metal permeability [mol/m s $Pa^{1/2}$], and δ is the membrane thickness [m]. The ratio P_M/δ is defined as the permeance. p_h and p_l are the total gas pressures [Pa] on the feed and permeate sides, respectively, and x_{N_2} and y_{N_2} are feed-side and permeate-side nitrogen mole fractions, respectively. It can be seen in Eq. (1) that the partial pressure on the feed side, $p_h x_{N_2}$, must be higher than that on the permeate side, $p_l y_{N_2}$, in order for the nitrogen flux from the feed to permeate side of the membrane to be positive. This would impose a constraint on the operating pressures used, i.e., p_h and p_l. A similar relationship was described in a study by Merkel and coworkers [7] for CO_2-selective membranes.

The membrane properties used in this study are listed in Table 2. The higher value of P_M is the permeability of hydrogen in vanadium at ca. 600 °C [27] and has been chosen as a benchmark for nitrogen transport in the materials of focus in the current study due to similarity in transport mechanisms. The lower value of P_M was calculated from the measurements of nitrogen transport in vanadium carried out by Özdoğan [21] and is in agreement with the permeability calculated from previous measurements of nitrogen diffusion in vanadium [28]. In Özdoğan's experiments, high

Table 2
Nitrogen- and CO_2-selective membrane properties.

Parameter	Value	Unit
Nitrogen-selective membrane		
Nitrogen permeability, P_M (high)	1×10^{-7}	mol/m s $Pa^{1/2}$
Nitrogen permeability, P_M (low)	5×10^{-13}	mol/m s $Pa^{1/2}$
Thickness, δ	10	μm
N_2/CO_2 selectivity	>1000	–
Operating temperature	600–900	°C
CO_2-selective membrane		
CO_2 permeance	1000	GPU[a]
CO_2/N_2 selectivity	50	–
Operating temperature	≤ 40	°C

[a] 1 GPU (gas processing unit) $= 3.35 \times 10^{-10}$ mol/m^2 s Pa.

operating temperatures were required for measureable nitrogen fluxes to diffuse across vanadium membrane foils [21]. The N_2/CO_2 selectivity was assumed to be >1000, similar to the H_2/CO_2 selectivity of dense metallic membranes for hydrogen separation when no structural defects are present [26]. The properties of the CO_2-selective membrane are based on the two-stage membrane separation unit available in IECM.

2.3. Membrane process designs

Six membrane process designs for the reference plant have been investigated. The process flow diagrams of these designs are shown in Fig. 2. The symbols used in the process diagrams are defined in Table 3. The capture unit can be installed either after the furnace or after the stack, depending on whether high-temperature flue gas is preferred. This will be discussed in detail later in this section. The designs with only nitrogen-selective membranes have been modeled for high and low nitrogen permeance scenarios as defined in Table 2. The benchmark value for nitrogen permeability, i.e., 1×10^{-7} mol/m s $Pa^{1/2}$, was used in the hybrid nitrogen- and CO_2-selective membrane processes.

The temperatures of the inlet streams to the compressors, vacuum pumps, and expanders were the decision variables within the model, thereby offering flexibility in the energy optimization, as the power consumption in both compression or expansion and heating or cooling is dependent on the stream temperature, as shown in Eqs. (3)–(5).

Feed compression in the single-stage or second-stage nitrogen-selective membrane is required by the positive flux constraint discussed previously. For the same reason, when the nitrogen-selective membrane is used in the first stage of a two-stage process, feed compression becomes optional. The designs that reflect this difference are Designs PC-2/PC-3 and Designs PC-4/PC-5. In Designs PC-2 and PC-4, the feed gas is cooled to a relatively low temperature and followed by compression. The compressed stream is reheated to 600 °C before entering the nitrogen-selective membrane. In Designs PC-3 and PC-5, the pressure difference in the first stage is created only by vacuum pumps. The high-temperature stream from the furnace is sent to the first-stage nitrogen-selective membrane, and no heating is needed. When the CO_2-selective membrane is used in the first stage, the flue gas, if at a high temperature, needs to be cooled down to the operating temperature range of the polymer-based membrane, as shown in Design PC-6.

In the designs with only nitrogen-selective membranes, CO_2 capture is essentially 100% from the assumption that minimal defects are present in the nitrogen-selective membrane. In the hybrid designs with both nitrogen- and CO_2-selective membranes, CO_2 capture was set to 90%. CO_2 product purity was set to 95% for all of the designs.

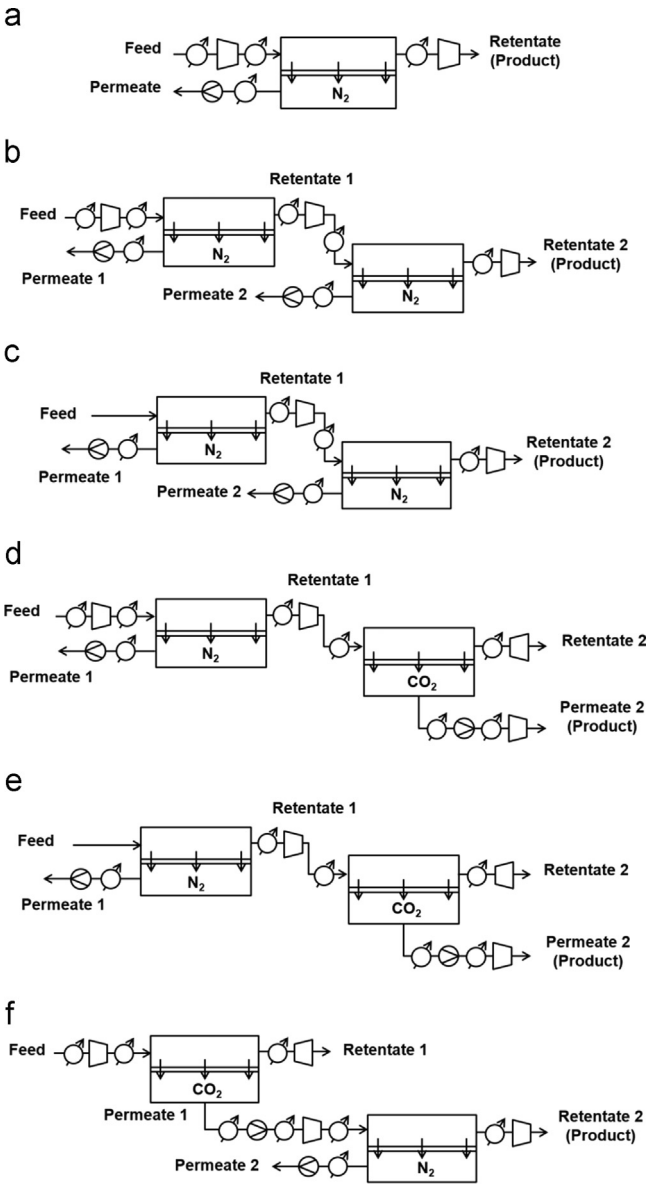

Fig. 2. Membrane process designs for the reference coal-fired power plant. Design PC-1 (a) is a single-stage nitrogen-selective membrane unit. Designs PC-2 (b) and PC-3 (c) are two-stage nitrogen-selective membranes. Designs PC-4 (d) and PC-5 (e) are two-stage units with the nitrogen-selective membrane in the first stage and CO_2-selective membrane in the second stage. Compression is applied on the first-stage feed in Designs PC-2 and PC-4, but not in Designs PC-3 and PC-5. Design PC-6 (f) is a two-stage unit with the CO_2-selective membrane in the first stage and nitrogen-selective membrane in the second stage.

Table 3
Definition of symbols used in process flow diagrams.

Compressor	
Vacuum pump	
Expander	
Heating or cooling unit	

Three-stage compression with intercooling was applied for all feed and product stream compression processes, with the product compressed up to 139 bar. It was also assumed that cooling from

Table 4
GA options used in this study.

Design	Pareto fraction	Crossover fraction	Population size	Generations
PC-1	0.5	0.7	50	70
PC-2	0.5	0.7	100	200
PC-3	0.5	0.7	100	100
PC-4	0.5	0.8	100	200
PC-5	0.5	0.9	100	150
PC-6	0.5	0.8	100	200

higher temperatures to as low as 30 °C does not incur additional energy use, and that the heat recovered from the process could be used for steam generation with minimal losses.

2.4. Modeling and optimization of membrane processes

To evaluate the true potential of nitrogen-selective membranes for industrial-scale CO_2 capture, rigorous optimization is required. The membrane modeling studies available in the literature mostly deal with single-objective optimization or parametric analysis with costs or energy consumption as the objective [7,8,12–14,16–19]. However, a capture plant should satisfy two criteria that have direct implications for operating and capital costs, namely low parasitic energy consumption and a small footprint. Thus, a multiobjective optimization showing the trade-off between the objectives would be essential for design and operation purposes. In the present study, the nondominated sorting genetic algorithm II (NSGA-II) proposed by Deb and coworkers [29] was used for multiobjective optimization. The algorithm is available in MATLAB's Global Optimization Toolbox. The optimizer minimized energy consumption and total membrane surface area simultaneously. The multiobjective GA options used for each design are listed in Table 4. The decision variables and their lower and upper bounds are listed in Table 5. A pressure of 0.2 bar was chosen to represent the lower pressure limit of large-scale industrial vacuum pumps due to practical considerations discussed in previous membrane modeling studies [7,15]. The dehydration temperature used in CO_2 compression in a DOE/NETL report on coal- and natural gas–fired power plants [30] has been chosen as the lower bound of the inlet temperature to compressors, vacuum pumps, and expanders. The positive flux requirement, i.e., the feed-side partial pressure must be higher than the permeate-side partial pressure, serves as another constraint on the stream pressures and compositions in all of the designs.

For a countercurrent flow pattern in an ideal, dense nitrogen-selective membrane, the required surface area, A [m^2] can be calculated by integrating Eq. (2) from the retentate-stream N_2 concentration, x_o, to the feed-stream N_2 concentration, x_f:

$$\frac{dA}{dx_{N_2}} = \frac{L_o(1-x_o)}{(1-x_{N_2})^2(P_{N_2}/\delta)(\sqrt{p_h x_{N_2}} - \sqrt{p_l})} \tag{2}$$

such that L_o is the retentate-stream flow rate [mol/s], and x_{N_2} is the N_2 mole fraction on the high-pressure side of the membrane and is a variable along the axial direction. Eq. (2) can be derived from Eq. (1) and the mass balance equations for a countercurrent flow pattern in a dense-phase, symmetric membrane as described in Geankoplis [25]. The derivation is outlined in the Appendix A.

The equation used for calculating the surface area of the polymeric, CO_2-selective membrane with a cross-flow flow pattern has been described elsewhere in the literature [25,31].

The power used in heating and cooling was calculated by Eq. (3), where $\dot{n}$ is the molar gas flow rate [mol/s], $C_{p,mix}$ is the mole-averaged constant-pressure specific heat [J/mol °C] of the gas stream, and ΔT is the temperature change [°C] of the gas stream. The efficiency of the heating and cooling processes, $\eta_{heating/cooling}$, was assumed to be 85%.

Table 5
Decision variables in this study.

Decision variable	Lower and upper limits
Feed pressure (if feed is compressed)	1–10 bar
Permeate pressure	0.2–1 bar
Temperatures of inlet streams to compressors, vacuum pumps, and expanders	−40 to 30 °C
Interim (first-stage) CO_2 purity	Satisfies the positive flux constraint

$$P_{heating/cooling} = \frac{\dot{n} C_{p,mix} \Delta T}{\eta_{heating/cooling}} \tag{3}$$

The compression power consumed by compressors and vacuum pumps can be calculated as [5,8,14,15]

$$P_{compression} = \frac{\dot{n}}{\eta_{equip}} \frac{kRT_{in}}{(k-1)} \left[\left(\frac{p_{out}}{p_{in}} \right)^{(k-1)/k} - 1 \right] \tag{4}$$

such that k is the heat capacity ratio, T_{in} is the inlet gas temperature [K], p_{in} and p_{out} are inlet and outlet stream pressures [bar], respectively, and η_{equip} is the equipment efficiency [%].

The power recovered by expanders can be calculated as [14]

$$P_{expansion} = \eta_{equip} \frac{\dot{n} k R T_{in}}{(k-1)} \left[1 - \left(\frac{p_{out}}{p_{in}} \right)^{(k-1)/k} \right] \tag{5}$$

In Eqs. (4) and (5), adiabatic processes were assumed, and the equipment efficiency of all compressors, vacuum pumps, and expanders was assumed to be 85%, with the exception of the product compressors, which was assumed to be 80%. The efficiencies are based on corresponding parameters in the CO_2-selective membrane unit in IECM.

3. Results

The Pareto curves showing the optimal ranges of required energy and membrane surface area are shown in Figs. 3 and 4. The energy penalty was defined to be the ratio of separation power consumption to gross generation of the reference plant. The energy use breakdown of all the process designs is shown in Table 6. The ratios of CO_2- to nitrogen-selective membrane surface area in the hybrid designs are listed in Table 7.

4. Discussion

In nitrogen-selective membrane processes, there exists a trade-off between the energy used for separation and the required membrane surface area. The same trend has been observed in separation processes with CO_2-selective membranes [14,15,18]. By comparing PC-2 and PC-3 results, it can be seen that the use of vacuum pumps on the permeate stream in the nitrogen-selective membrane lowers compression energy use, similar to CO_2-selective membrane processes and as expected. However, vacuum pumping plays a less direct role in reducing compression energy in nitrogen-selective membranes than in CO_2-selective membranes. In the latter, vacuum pumping is applied to the CO_2-rich permeate stream, which is about one-tenth of the feed flow rate. Less energy is consumed because a gas stream of a much smaller flow rate is compressed. In contrast, in nitrogen-selective membranes, vacuum pumping is applied to nitrogen streams having flow rates comparable to those of feed streams. Nevertheless, vacuum pumping contributes to the reduction of separation

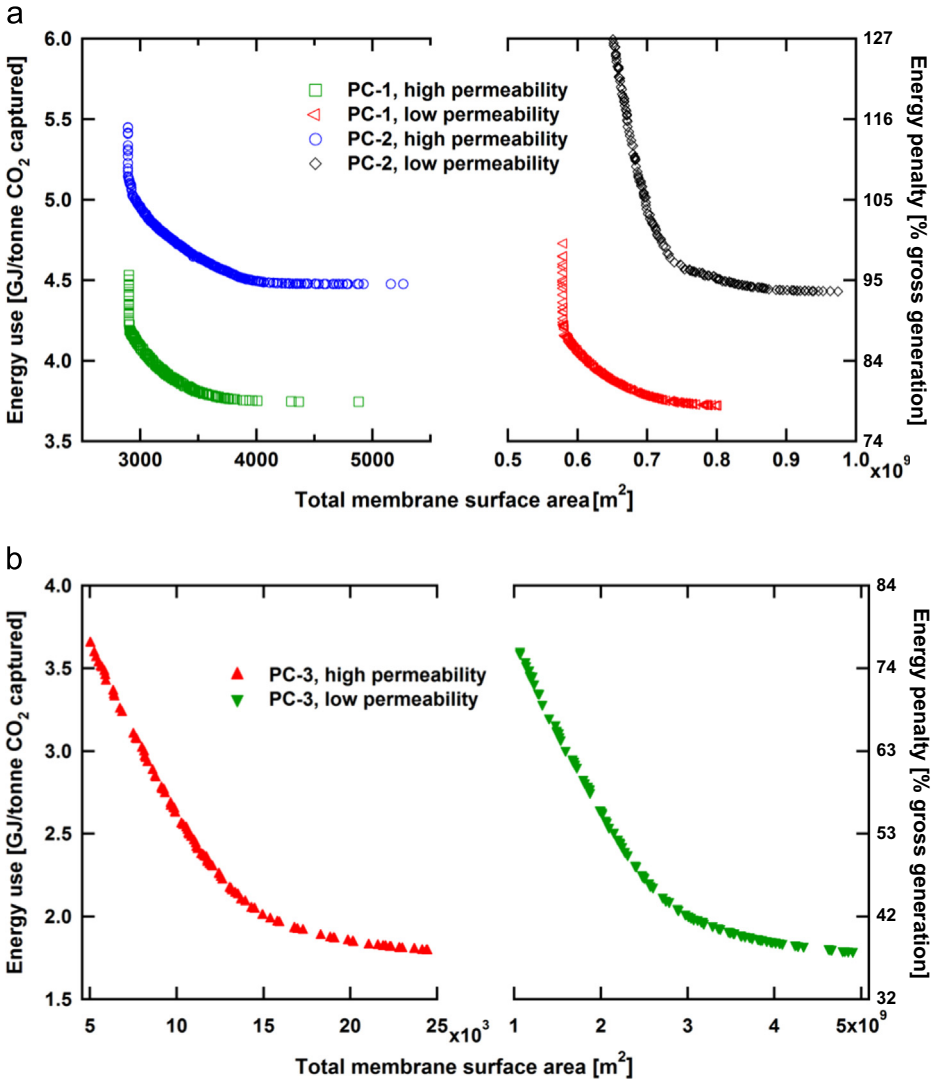

Fig. 3. Pareto curves of (a) Designs PC-1 and PC-2 and (b) Design PC-3. The high permeability scenario corresponds to a nitrogen permeability of 1×10^{-7} mol/m s $Pa^{1/2}$, and the low permeability scenario corresponds to 5×10^{-13} mol/m s $Pa^{1/2}$. All the three designs achieved 100% capture and 95% purity of CO_2. 1 tonne = 1 metric ton.

energy by allowing the high-temperature feed to be sent to the separation unit, thus eliminating cooling and heating use associated with feed compression. This can be seen by comparing the heating and cooling power (in MW) of PC-2 with PC-3 and PC-4 with PC-5 in Table 6.

Targets of $>90\%$ capture and 95% CO_2 purity can be simultaneously achieved in the nitrogen-selective membrane in a single stage. However, from the modeling results, it can be seen that the application of this technology in large-scale postcombustion capture processes is constrained by both energy use and membrane surface area. For postcombustion capture from the PC plant, the separation energy use is not sufficiently competitive with that of other proposed capture technologies. The optimal range of energy use is 2–5 GJ/metric ton using nitrogen-selective membranes alone. In comparison, the separation energy use of absorption is in the range of 3–4 GJ/metric ton CO_2 [4]. Typical energy use of CO_2-selective membranes is approximately 1–3 GJ/metric ton CO_2 based on the modeling results in the literature [7,8,10,12–20]. Direct comparison of the three systems requires caution. Absorption primarily uses heat, a low-value form of energy, whereas membrane separation consumes electricity [5,19]. The nitrogen-selective membrane uses a mix of electric and thermal energy. Although numerical conversion between electric and thermal energy is possible in general, such conversion for the nitrogen-selective membrane in the context of carbon capture would be complicated by factors such as the effectiveness of heat integration, the energy sources available and the associated emission factors.

As shown in Table 6, a large proportion of the energy use in nitrogen-selective membranes is for cooling and heating, which is required by feed-stream compression and the high operating temperature of the nitrogen-selective membrane. Although thermal energy is of lower value compared to electricity, an improved heat exchanger network design, with the possibility of concurrent stream recycling, should be contemplated to reduce the cooling and heating use if the nitrogen-selective membrane is to be used in large-scale capture processes. In addition, it may be useful to work toward the design and development of nitrogen-selective membrane materials that require lower operating temperatures.

Design PC-5, where the nitrogen-selective membrane acts as a CO_2 enricher, has shown potential for being as energy-efficient as the CO_2-selective membrane systems described in the literature. Such a design may become a niche application for nitrogen-selective membranes in postcombustion capture, especially when flue gas CO_2 concentration is too low for CO_2-selective membranes to be effective, such as in a natural gas combined-cycle.

In view of current permeability measurements, the required membrane surface area of the nitrogen-selective membrane would

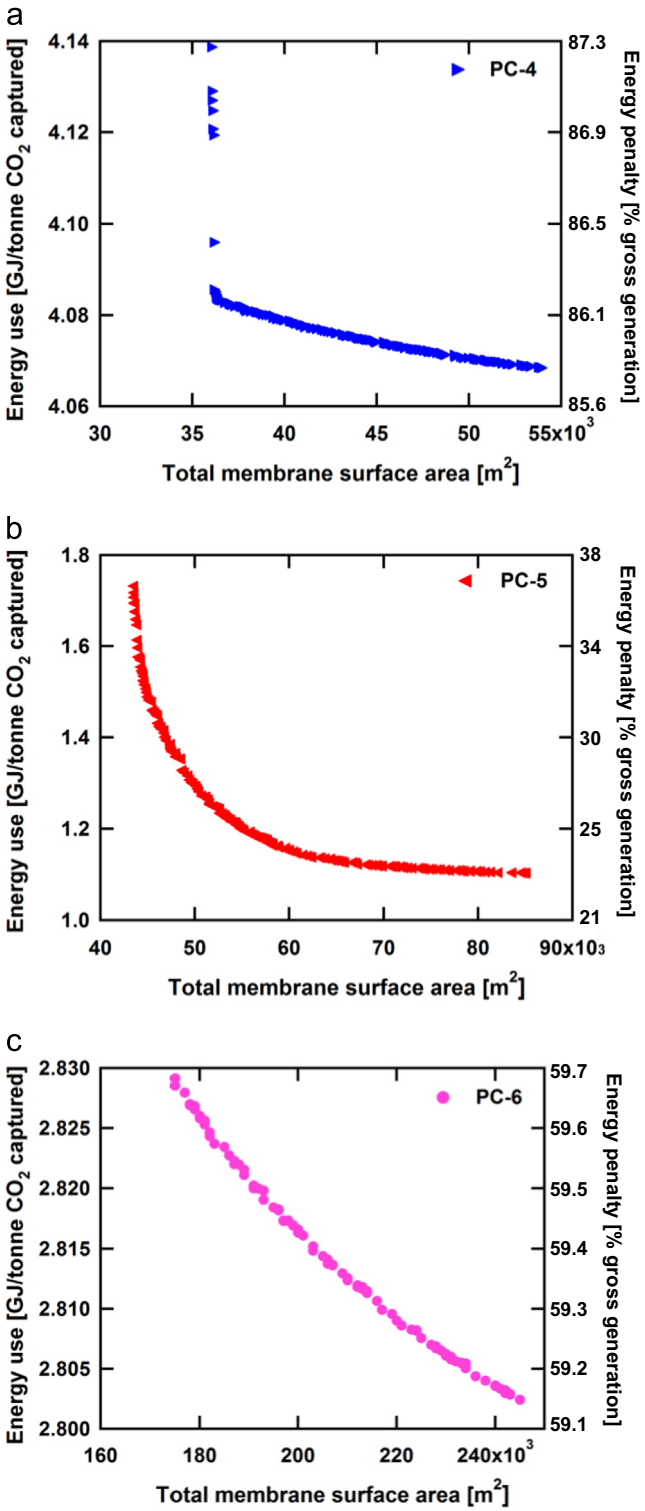

Fig. 4. Pareto curves of (a) Design PC-4, (b) Design PC-5, and (c) Design PC-6. Nitrogen permeability was assumed to be 1×10^{-7} mol/m s $Pa^{1/2}$ for all the three designs. The CO_2-selective membrane had a permeance of 1000 GPU and CO_2/N_2 selectivity of 50. Separation targets were 90% capture and 95% purity. 1 tonne = 1 metric ton.

be too high for large-scale applications. In comparison, the required surface area of CO_2-selective membranes for capture at similar scales is on the order of 10^5–10^7 m^2 [7,10–12,14–20]. Indeed, membrane surface area is not the only indication of the final capture plant size. The land use of the capture plant is also dependent on the surface area–to-volume ratio of the membrane. However, capital cost may become an important concern if the

Table 6
Power use breakdown by component.

Design	Feed and permeate compr. [%]	Product compr. [%]	Heating and cooling [%]	Expander recovery [%]	Total power [MW]
PC-1, high perm.	38–44	4–5	51–57	–	514–621
PC-1, low perm.	38–45	4–5	50–58	–	510–648
PC-2, high perm.	28–36	4–5	60–67	–	614–747
PC-2, low perm.	22–27	2–5	69–76	–	608–1140
PC-3, high perm.	38–46	5–11	44–57	–	244–570
PC-3, low perm.	37–46	5–11	44–58	–	243–577
PC-4	30–31	10	60–61	2	502–512
PC-5	60–68	23–39	6–21	5–6	136–214
PC-6	44–48	9–10	54–57	10–11	346–349

Table 7
Surface area ratios of CO_2– to nitrogen-selective membranes.

Design	Ratio
PC-4	11–17
PC-5	1–3
PC-6	108–186

metallic membranes used for nitrogen separation are more expensive than polymeric membranes per unit surface area. It can be seen by comparing the high- and low-permeability scenarios that low nitrogen permeability significantly increases the required membrane surface area, although the variations in permeability do not greatly change the calculated optimal ranges of energy use. In addition to enhancing nitrogen permeability in the membrane materials, the development of thinner membranes will reduce the required membrane surface area by increasing the permeance (i.e., mass-transfer coefficient) and consequently the nitrogen flux. The reduction in membrane thickness will also reduce the amount of membrane material used for the same surface area required, which may further reduce the cost of the membrane. An example of an ultrathin metallic membrane can be found in a recent article, in which the reported thickness of a pure palladium membrane is 0.93 μm [32]. Although reducing the membrane thickness is just as important as increasing the permeability, there are physical limitations associated with reduced thickness such as more defects and lower stability.

In the optimization of hybrid membrane systems, the summation of the surface areas in the first and second stages was considered as one of the objective functions. This essentially means that equal weight was assigned to the two membranes, and an underlying assumption is that the two membranes have comparable scale-up potentials and that the modules occupying the same land area would have similar costs. This assumption is subject to change in cases where one type of membrane is preferred for its lower energy use or smaller land use than the other.

An observation on the optimized compressor, vacuum pump, and expander inlet temperatures may offer some insight into the workings of the optimizer. The lower bound of temperatures (Table 5) was initially set to a low value with the intent that the compression energy would be optimized by varying the inlet temperature. However, the optimized inlet temperatures that correspond to the optimal energy–membrane surface area points on the Pareto curves in Figs. 3 and 4 mostly remained above 0 °C, indicating that the optimization resulted from a balance of (a) compression energy use and heating and cooling use and

(b) the two objective functions, i.e., the total energy consumption and the membrane surface area. That is to say, the bi-objective optimizer strives for a strategy that achieves the overall minimization.

In this modeling work, it was assumed that nitrogen only permeates through the membrane via a solution–diffusion mechanism. At the current stage of development, however, defects may be present in the membrane materials, allowing for the passage of CO_2 as well as nitrogen via Knudsen diffusion. In addition, other components such as O_2, SO_2, and water vapor in the flue gas may compromise the membrane materials through oxidation, sulfurization, and other reactions under flue gas conditions. Future work will investigate the oxidant- and sulfur-resistance of the membrane materials. Oxidant removal and desulfurization will also likely be considered along with heat integration as an improvement to the current process design. In general, real material properties and flue gas conditions and other non-idealities need to be incorporated in future modeling studies and should be addressed initially at the lab scale if industrial-scale carbon capture is one of the applications envisioned for a nitrogen-selective membrane technology.

5. Conclusions

This modeling study investigated the possibility of applying a metallic nitrogen-selective membrane to postcombustion carbon capture from a coal-fired power plant. Capture and purity targets of $>90\%$ capture and 95% CO_2 purity can be obtained simultaneously in the nitrogen-selective membrane in a single stage. When the nitrogen-selective membrane is used as a feed CO_2 enricher, the design has the potential to compete with other capture technologies described in the literature in terms of energy use. However, some key issues need to be addressed before the membrane can be used under real flue gas conditions on an industrial scale.

- Energy consumption by heating and cooling, which is required by the high operating temperature of the membrane, needs to be lowered. This will require efforts in both process design and material development.
- Membrane permeance needs to be significantly improved to lower the required membrane surface area for separation. This can be achieved by improving nitrogen transport and/or by reducing the membrane thickness. The nitrogen-selective membrane would potentially be able to compete with CO_2-selective membranes in terms of land use if the permeance were to be lowered by at least 2–3 orders of magnitude from the current range.
- The effects of other components, e.g., O_2, SO_2, and water vapor, in the flue gas will need to be investigated in both laboratory and modeling studies.

Acknowledgments

The authors would like to thank the Division of Chemical, Bioengineering, Environmental, and Transport Systems of the National Science Foundation (Award #1263991) for financial support for the project. In addition, Dr. Haibo Zhai, Dr. Edward Rubin, and Dr. Stephen Paglieri are acknowledged for their guidance and helpful suggestions throughout the course of this study.

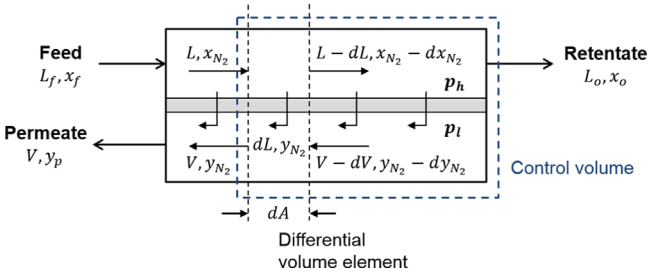

Fig. A.1. Schematic diagram of countercurrent flow pattern across a dense nitrogen-selective membrane.

Appendix A

Derivation of membrane surface area required for separation using an ideal, dense nitrogen-selective membrane.

The schematic diagram of a countercurrent flow pattern across the membrane is shown in Fig. A.1.

The overall flow balance and mass balance on nitrogen on the control volume is

$$L = L_0 + V \tag{A.1}$$

$$Lx_{N_2} = L_o x_o + V y_{N_2} \tag{A.2}$$

such that L and V are molar flow rates of streams entering and leaving the left-side boundary of the control volume, respectively, and L_0 is the molar flow rate of the retentate stream. x_{N_2}, y_{N_2}, and x_o are nitrogen mole fractions associated with L, V, and L_0, respectively.

Under the assumption of an ideal nitrogen-selective membrane, $y_{N_2} = 1$. Combining Eqs. (A.1) and (A.2) and rearranging:

$$L = \frac{L_o(1-x_o)}{1-x_{N_2}} \tag{A.3}$$

The nitrogen flux permeated across the membrane can be calculated by combining Fick's first law and Sieverts' law:

$$J_{N_2} = \frac{dL_{N_2}}{dA} = \frac{d(y_{N_2}L)}{dA} = \frac{P_M}{\delta}\left(\sqrt{p_h x_{N_2}} - \sqrt{p_l y_{N_2}}\right) \tag{A.4}$$

such that L_{N_2} is the nitrogen flow rate passing through the membrane. Since $y_{N_2} = 1$, $L_{N_2} = L$. Eq. (A.4) becomes

$$J_{N_2} = \frac{dL}{dA} = \frac{P_M}{\delta}\left(\sqrt{p_h x_{N_2}} - \sqrt{p_l}\right) \tag{A.5}$$

Mass balance on nitrogen on the differential volume element is

$$Lx_{N_2} = (L - dL)(x_{N_2} - dx_{N_2}) + y_{N_2}\, dL \tag{A.6}$$

Rearranging Eq. (A.6), invoking $y_{N_2} = 1$, and neglecting the term $dL\, dx_{N_2}$:

$$L\, dx_{N_2} = (1 - x_{N_2})dL \tag{A.7}$$

Combining Eq. (A.7) with Eqs. (A.3) and (A.5) and rearranging:

$$\frac{dA}{dx_{N_2}} = \frac{L_o(1-x_o)}{(1-x_{N_2})^2(P_{N_2}/\delta)\left(\sqrt{p_h x_{N_2}} - \sqrt{p_l}\right)} \tag{A.8}$$

References

[1] S. Solomon, G.-K. Plattner, R. Knutti, P. Friedlingstein, Irreversible climate change due to carbon dioxide emissions, Proc. Natl. Acad. Sci. 106 (2009) 1704–1709.
[2] J. Gillis, Heat-trapping Gas Passes Milestone, Raising Fears, New York Times, New York, NY, 2013.
[3] J. Wilcox, Carbon Capture, Springer, New York, NY, 2012.
[4] Working Group III of the Intergovernmental Panel on Climate Change, in: B. Metz, O. Davidson, H. de Coninck, M. Loos, L. Meyer (Eds.), IPCC Special Report on Carbon Dioxide Capture and Storage, Cambridge University Press, New York, 2005.

[5] E. Favre, Carbon dioxide recovery from post-combustion processes: can gas permeation membranes compete with absorption? J. Membr. Sci. 294 (2007) 50–59.
[6] J.D. Figueroa, T. Fout, S. Plasynski, H. McIlvried, R.D. Srivastava, Advances in CO_2 capture technology—the US Department of Energy's Carbon Sequestration Program, Int. J. Greenh. Gas Control 2 (2008) 9–20.
[7] T.C. Merkel, H. Lin, X. Wei, R. Baker, Power plant post-combustion carbon dioxide capture: an opportunity for membranes, J. Membr. Sci. 359 (2010) 126–139.
[8] R. Bounaceur, N. Lape, D. Roizard, C. Vallieres, E. Favre, Membrane processes for post-combustion carbon dioxide capture: a parametric study, Energy 31 (2006) 2556–2570.
[9] A. Brunetti, F. Scura, G. Barbieri, E. Drioli, Membrane technologies for CO_2 separation, J. Membr. Sci. 359 (2010) 115–125.
[10] J. Franz, S. Schiebahn, L. Zhao, E. Riensche, V. Scherer, D. Stolten, Investigating the influence of sweep gas on CO_2/N_2 membranes for post-combustion capture, Int. J. Greenh. Gas Control 13 (2013) 180–190.
[11] M.-B. Hägg, A. Lindbråthen, CO_2 capture from natural gas fired power plants by using membrane technology, Ind. Eng. Chem. Res. 44 (2005) 7668–7675.
[12] M.T. Ho, G.W. Allinson, D.E. Wiley, Reducing the cost of CO_2 capture from flue gases using membrane technology, Ind. Eng. Chem. Res. 47 (2008) 1562–1568.
[13] J. Van Der Sluijs, C. Hendriks, K. Blok, Feasibility of polymer membranes for carbon dioxide recovery from flue gases, Energy Convers. Manage. 33 (1992) 429–436.
[14] D. Yang, Z. Wang, J. Wang, S. Wang, Potential of two-stage membrane system with recycle stream for CO_2 capture from postcombustion gas, Energy Fuels 23 (2009) 4755–4762.
[15] H. Zhai, E.S. Rubin, Techno-economic assessment of polymer membrane systems for postcombustion carbon capture at coal-fired power plants, Environ. Sci. Technol. 47 (2013) 3006–3014.
[16] L. Zhao, R. Menzer, E. Riensche, L. Blum, D. Stolten, Concepts and investment cost analyses of multi-stage membrane systems used in post-combustion processes, Energy Proc. 1 (2009) 269–278.
[17] L. Zhao, E. Riensche, L. Blum, D. Stolten, Multi-stage gas separation membrane processes used in post-combustion capture: energetic and economic analyses, J. Membr. Sci 359 (2010) 160–172.
[18] L. Zhao, E. Riensche, L. Blum, D. Stolten, How gas separation membrane competes with chemical absorption in postcombustion capture, Energy Proc. 4 (2011) 629–636.
[19] L. Zhao, E. Riensche, R. Menzer, L. Blum, D. Stolten, A parametric study of CO_2/N_2 gas separation membrane processes for post-combustion capture, J. Membr. Sci. 325 (2008) 284–294.
[20] L. Zhao, E. Riensche, M. Weber, D. Stolten, Cascaded membrane processes for post-combustion CO_2 capture, Chem. Eng. Technol. 35 (2012) 489–496.
[21] E. Özdoğan, Theoretical and Experimental Investigations of Metallic Membranes for CO_2 Capture (Ph.D. thesis), Department of Energy Resources Engineering, Stanford University, Stanford, CA, 2012.
[22] Integrated Environmental Control Model, Carnegie Mellon University, ⟨http://www.cmu.edu/epp/iecm/index.html⟩.
[23] Steam, Its Generation and Use, 41st ed., The Babcock & Wilcox Company, Barberton, OH, 2005.
[24] F. Gallucci, M. van Sint Annaland, J.A.M. Kuipers, Modeling of membrane reactors for hydrogen production and purification, in: E. Drioli, G. Barbieri (Eds.), Membrane Engineering for the Treatment of Gases, Volume 2: Gas-separation Problems Combined with Membrane Reactors, Royal Society of Chemistry, Cambridge, UK, 2011.
[25] C. Geankoplis, Transport Processes and Separation Process Principles, 4th ed., Prentice Hall Press, Upper Saddle River, NJ, 2003.
[26] DOE/NETL, Integration of H_2 separation Membranes with CO_2 Capture and Compression, DOE/NETL-401/113009, 2009.
[27] R.E. Buxbaum, A.B. Kinney, Hydrogen transport through tubular membranes of palladium-coated tantalum and niobium, Ind. Eng. Chem. Res. 35 (1996) 530–537.
[28] J. Keinonen, J. Räisänen, A. Anttila, Diffusion of nitrogen in vanadium and niobium, Appl. Phys. A Mater. Sci. Process. 34 (1984) 49–56.
[29] K. Deb, A. Pratap, S. Agarwal, T. Meyarivan, A fast and elitist multiobjective genetic algorithm: NSGA-II, IEEE Trans. on Evol. Comput. 6 (2002) 182–197.
[30] DOE/NETL, Cost and performance baseline for fossil energy plants, Volume 1: Bituminous Coal and Natural Gas to Electricity, Revision 2, DOE/NETL-2010/1397, 2010.
[31] H. Zhai, E.S. Rubin, IECM Technical Documentation: Membrane-based CO_2 Capture Systems for Coal-fired Power Plants, Carnegie Mellon University, Pittsburgh, PA, 2012.
[32] Ø. Hatlevik, S.K. Gade, M.K. Keeling, P.M. Thoen, A. Davidson, J.D. Way, Palladium and palladium alloy membranes for hydrogen separation and production: history, fabrication strategies, and current performance, Sep. Purif. Technol. 73 (2010) 59–64.